Supporting Information

Molecular Weight-regulated Sequential Deposition Strategy Enables Semitransparent Organic Solar Cells with Light Utilization Efficiency over 5%

Xuexiang Huang[a, 1], Yujun Cheng[a, 1] Yuan Fang[d], Lifu Zhang[b, 1], Xiaotian Hu[a], Sang Young Jeong[c], Hean Zhang[a], Han Young Woo[c], Feiyan Wu[a], Lie Chen[a,*]

[a] *Institute of Polymers and Energy Chemistry (IPEC)/College of Chemistry and Chemical Engineering, Nanchang University, Nanchang 330031, Jiangxi, China*

[b] *Institute of Advanced Scientific Research (iASR)/Key Lab of Fluorine and Silicon for Energy Materials and Chemistry of Ministry of Education, Jiangxi Normal University, Nanchang 330022, China*

[c] *S. Y. Jeong, Prof. H. Y. Woo Department of Chemistry College of Science Korea University 145 Anam-ro, Seongbuk-gu, Seoul 02841, Republic of Korea*

[d] *School of Future Technology, Nanchang University, Nanchang 330036, Jiangxi China*

[*]**Corresponding authors.**

Email addresses: chenlie@ncu.edu.cn (L. Chen)

[1] These authors contributed equally to this work.

1. Materials and synthesis

BDT-2F and F-TT was purchased from Derthon Optoelectronic Materials Science Technology Co LTD (Shenzhen, China). All reagents and commercially available compounds are used upon receipt. The synthetic processes of two series of random copolymers are provided in **Figure S1**. The synthesis of polymer PCE10-2F is as follows:

BDT-2F (181 mg, 0.2 mmol), F-TT (94.4 mg, 0.2 mmol) and Pd $(PPH_3)_4$ (18.5 mg, 0.016 mmol) were dissolved in mixed solvents (toluene (5 ml) and DMF (1 ml) in nitrogen atmosphere in a 50 ml double-necked flask with condenser. Mix the mixture for 9-16 hours (PCE10-2F-33.4kDa for 9 hours, PCE10-2F-40.8kDa for 11 hours, PCE10-2F-53.3kDa for 14 hours and 61.1kDa for 16 hours) at 120℃. After cooling the solution to room temperature, it is poured into methanol (300 ml). The precipitation was collected by filtration, and then the product was further purified by Soxhlet extraction. The product was extracted with n-hexane, acetone and $CHCl_3$ for one day in turn. PCE10-2F were dissolved in $CHCl_3$ and precipitated with methanol. Finally, it is collected by filtration and dried in a vacuum oven at 80℃ for more than 20 hours. PCE10-2F were obtained in the form of dark blue solids.

Measurements

Optical absorption spectra of the polymers were measured on a PerkinElmer model Lambda 900 UV-vis/near-IR spectrophotometer. Solution and solid-state absorption spectra were obtained from dilute (10^{-6} M) polymer solution in chloroform and from thin films on glass substrate, respectively. Thin films were spin coated from 20 mg/mL solutions in chloroform.

Washing process: The polymer donor PCE10-2F was dissolved in chloroform (CF) at a concentration of 8 mg/ml, the solution was stirred at 40 °C for 10 h, and then spin-coated on the quartz substrate surface in a glove box under nitrogen atmosphere (2000 r 40 s). Then the optical absorption spectra of the polymers were measured on a PerkinElmer model Lambda 900 UV-vis/near-IR spectrophotometer. Next, the sample was taken out, and pure chloroform (12 uL) was spin-coated at 2300r/min for 40s and the optical absorption spectra of the polymers after pure chloroform washing was measured on a PerkinElmer model Lambda 900 UV-vis/near-IR spectrophotometer.

The specimen for atomic force microscopy (AFM) measurements was prepared using the same procedures those for fabricating devices but without PDINO/Ag on top of the active layer. Transmission electron microscope (TEM) images were taken on a JEOL-2100F transmission electron microscope and an internal charge-coupled device (CCD) camera. The specimen for TEM measurement was prepared by spin casting the blend solution on ITO/PEDOT: PSS substrate, then floating the film on a water surface, and transferring to TEM grids.

The GIWAXS measurement was carried out at the PLS-II 6A U-SAXS beamline of the Pohang Accelerator Laboratory in Korea. The X-rays coming from the in-vacuum undulator (IVU) were monochromated (wavelength λ = 1.10994 Å) using a double crystal monochromator and focused both horizontally and vertically (450 (H) x 60 (V) um^2 in FWHM @ the sample position) using K-B type mirrors. The grazing incidence wide-angle X-ray scattering (GIWAXS) sample stage was equipped with a 7-axis motorized stage for the fine alignment of the sample, and the incidence angles of the X-ray beam were set to be 0.11°-0.13° for the neat and blend films. The GIWAXS patterns were recorded with a 2D CCD detector (Rayonix SX165) and an X-ray irradiation time within 100 s, dependent on the saturation level of the detector. Diffraction angles were calibrated using a sucrose standard (monoclinic, P21, a=10.8631Å, b =8.7044Å, c=7.7624Å, and b=102.938Å) and the sample-to-detector distance was ~231 mm.

2. Device fabrication

2.1 Opaque device fabrication

The device is fabricated with ITO/PEDOT:PSS/active layer/PDINO/Ag tradition structure. The ITO coated glass substrates were cleaned by ultrasound for 15 minutes in sequence in water/detergent, water, acetone and isopropanol, and then treated in ultraviolet-ozone for 1400 seconds. The PEDOT:PSS solution was spin-coated on top of the cleaned ITO-coated glass substrate and the PEDOT:PSS film thickness was approximately 25 nm. After annealing at 150 °C for 20 min, then the substrates were transferred into a glove box. For the solar cells based on a BC operating condition, polymer doner: Y6 (1:2, w/w) mixture was dissolved in chloroform (CF) with a

concentration of 16 mg/ml, and 1,8-diiodooctane (DIO) and CN was added (volume ratio 0.25% and 0.25%, respectively). The solution is stirred at 40℃ for 10 hours and then spin-coated on the surface of PEDOT:PSS layer in a glove box in nitrogen-based atmosphere (3000r 40s). After annealing at 100 °C for 10 min. For the solar cells based on a SD operating condition, PCE10-2F with a concentration of 8 mg mL^{-1} in CF were spun onto the PEDOT: PSS layers at 2500 rpm (60 nm), 4000 rpm (50 nm) or 5500 rpm (40 nm) for 40 s form the front layer, Y6 with a concentration of 10 mg mL^{-1} in CF, and 1,8-diiodooctane (DIO) and CN was added (volume ratio 0.25% and 0.25%, respectively). then spun onto the PCE10-2F layers at 2300 rpm (40nm) for 40 s. After annealing at 100 °C for 10 min. The PDINO was dissolved in methanol at 3 mg mL^{-1} and spin-coated on active layer at 3000 rpm for 30s. Finally, 90-nanometer thick Ag layers were deposited on the active layer under high vacuum of ~$3x10^{-4}$Pa. The overlapping area of cathode and anode was 4 square millimeters. J-V curves of devices based on polymer doner: Y6 were measured under the standard AM 1.5G spectrum of 100 MW cm^{-2}.

2.2 Semitransparent device fabrication

The device is fabricated with ITO/PEDOT:PSS/active layer/PDINO-3/Ag tradition structure. The ITO coated glass substrates were cleaned by ultrasound for 15 minutes in sequence in water/detergent, water, acetone and isopropanol, and then treated in ultraviolet-ozone for 1400 seconds. The PEDOT:PSS solution was spin-coated on top of the cleaned ITO-coated glass substrate and the PEDOT:PSS film thickness was approximately 25 nm. After annealing at 150 °C for 20 min, then the substrates were transferred into a glove box. PCE10-2F-53.3kDa with a concentration of 8 mg mL^{-1} in CF were spun onto the PEDOT: PSS layers at 2500 rpm (60 nm), 4000 rpm (50 nm) or 5500 rpm (40 nm) for 40 s form the front layer, Y6 with a concentration of 10 mg mL^{-1} in CF, and 1,8-diiodooctane (DIO) and CN was added (volume ratio 0.25% and 0.25%, respectively). then spun onto the PCE10-2F layers at 2300 rpm (40 nm) for 40 s. After annealing at 100 °C for 10 min. The PDINO was dissolved in methanol at 3 mg mL^{-1} and spin-coated on active layer at 3000 rpm for 30s. Finally, 15nm thickness

Ag and layers were deposited on the active layer under high vacuum of ~3x10^{-4}Pa. Then, MoO_3 (35 nm) were evaporated onto the surface of Ag. The overlapping area of cathode and anode was 4 square millimeters. J-V curves of ST-OSC devices were measured under the standard AM 1.5G spectrum of 100 MW cm^{-2}.

3. Optical Characterization

The average visible transmittance (AVT) is calculated using

$$VLT = \frac{\int T(\lambda)P(\lambda)S(\lambda)d(\lambda)}{\int P(\lambda)S(\lambda)d(\lambda)} VLT = \frac{\int T(\lambda)P(\lambda)S(\lambda)d(\lambda)}{\int P(\lambda)S(\lambda)d(\lambda)}$$

$$AVT = \frac{\int T(\lambda)V(\lambda)S(\lambda)d(\lambda)}{\int P(\lambda)S(\lambda)d(\lambda)} \quad \text{(Eq. S1)}$$

where λ is the wavelength, T is the transmission, V is the normalized photopic spectral response of the eye, and S is the solar photon flux (AM1.5G). It is estimated by taking the average of the transparency of the devices in the visible region (380-740 nm) based on the photonic response of the human eye.

All the photographs are taken by Apple iPhone13 Pro.

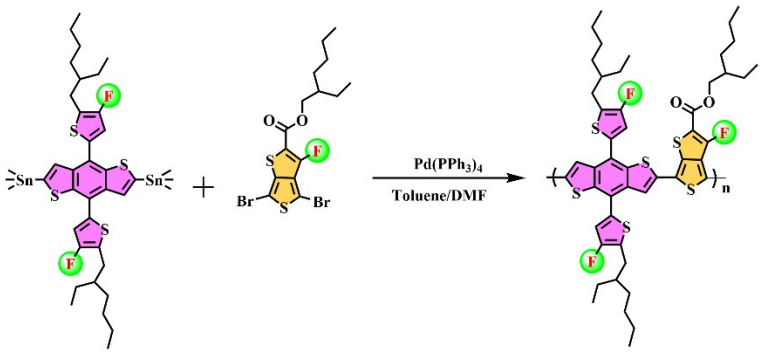

Figure S1. The synthetic route of PCE10-2F.

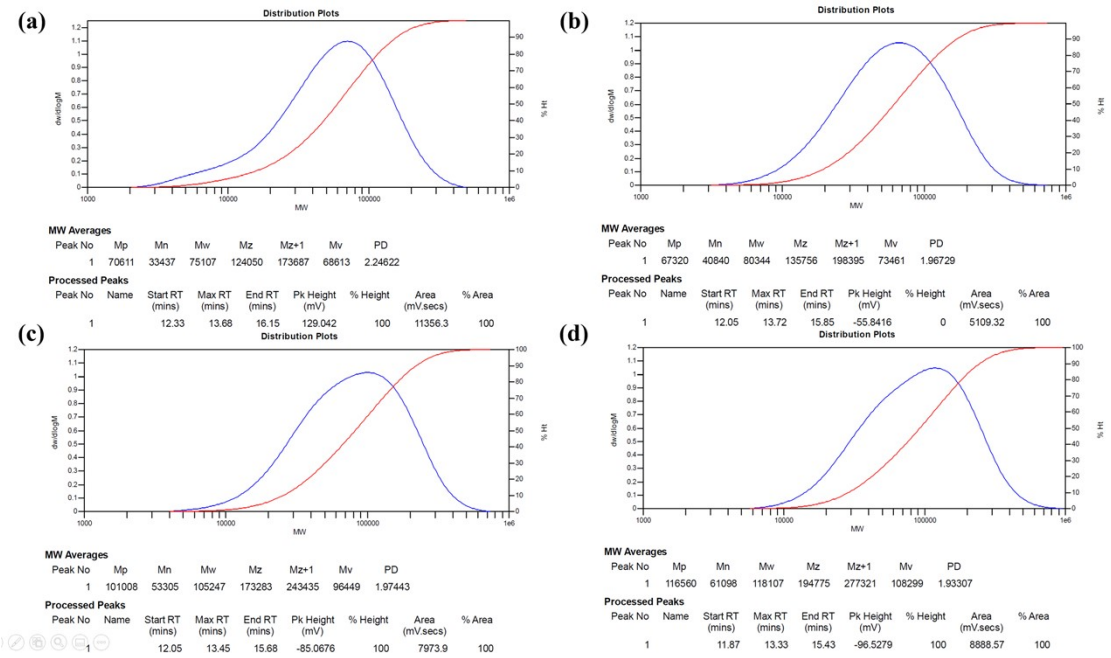

Figure S2. GPC peak report for PCE10-2F-32.4 kDa, PCE10-2F-40.8 kDa, PCE10-2F-53.3 kDa and PCE10-2F-61.1 kDa.

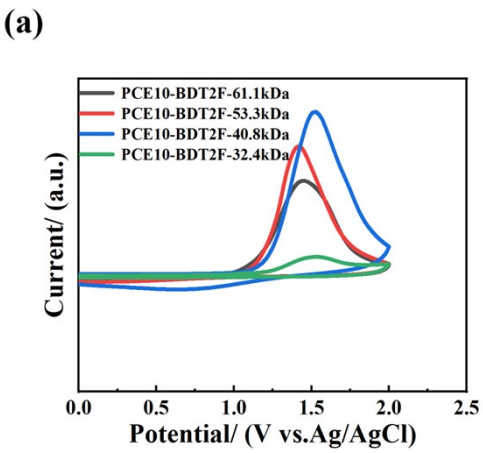

Figure S3. (a) CV curves of PCE10-2F-32.4kDa, PCE10-2F-40.8kDa, PCE10-2F-53.3kDa and PCE10-2F-61.1kDa.

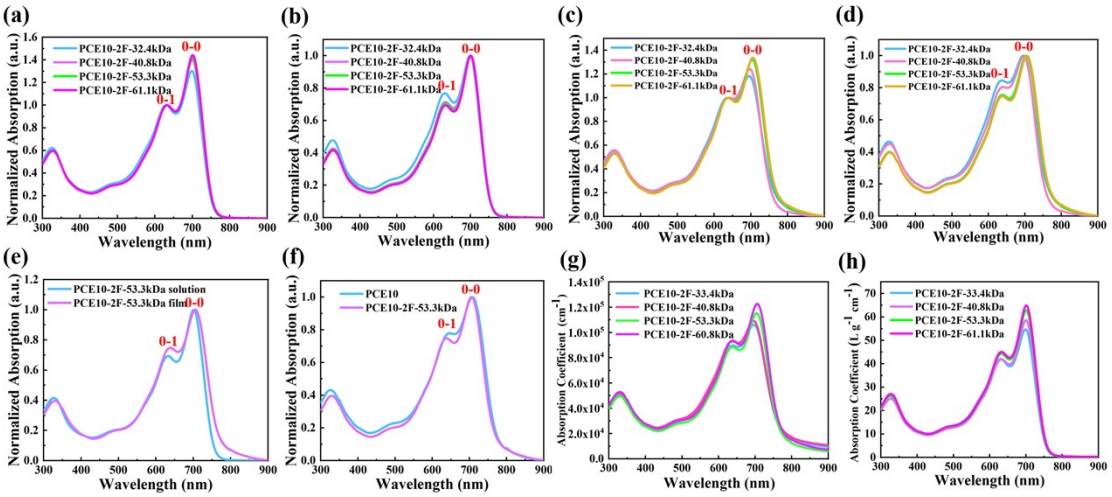

Figure S4. UV-vis absorption spectra of PCE10-2F-32.4kDa, PCE10-2F-40.8kDa, PCE10-2F-53.3kDa and PCE10-2F-61.1kDa were measured in (a-b) chlorobenzene solutions and (c-d) films. (e) UV-vis absorption spectra of PCE10-2F-53.3kDa were measured in chlorobenzene solutions and films, respectively. (f) UV-vis absorption spectra of PCE10-2F-53.3kDa and PCE10 were measured in films. (g) Absorption coefficients of the pristine polymers films. (h) absorption coefficient of pristine polymers in CB solution.

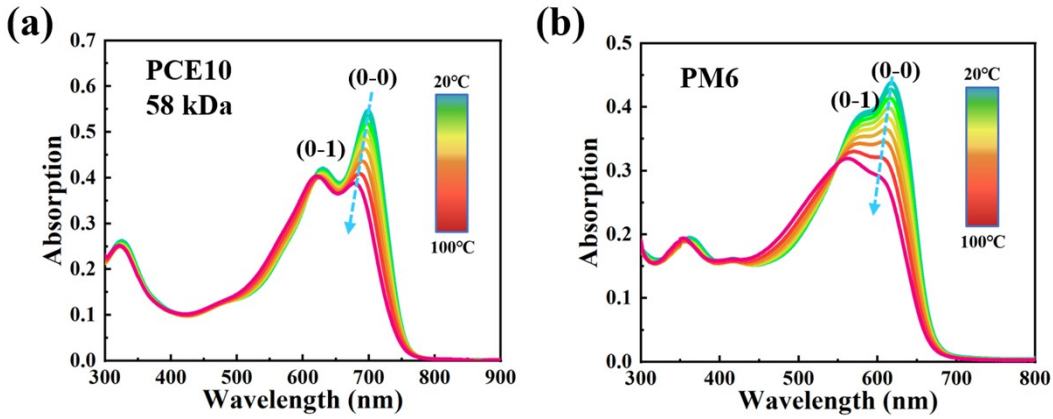

Figure S5. Temperature-dependent UV-vis absorption spectra of 0.01 mg/mL (a) PCE10 and (b) PM6 in CB.

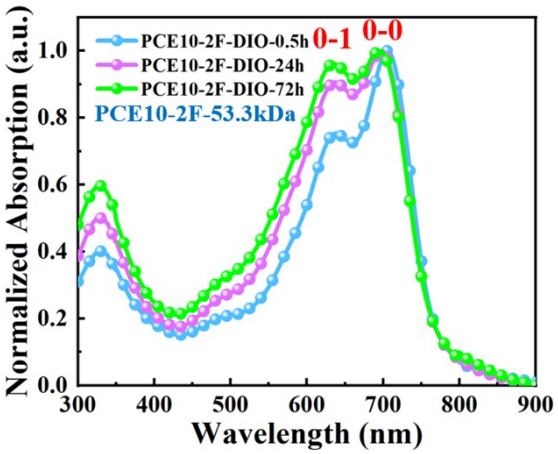

Figure S6. Normalized absorption spectra of PCE10-2F-53.3 kDa film after treatment with DIO additive for 0.5 h, 24 h and 72 h.

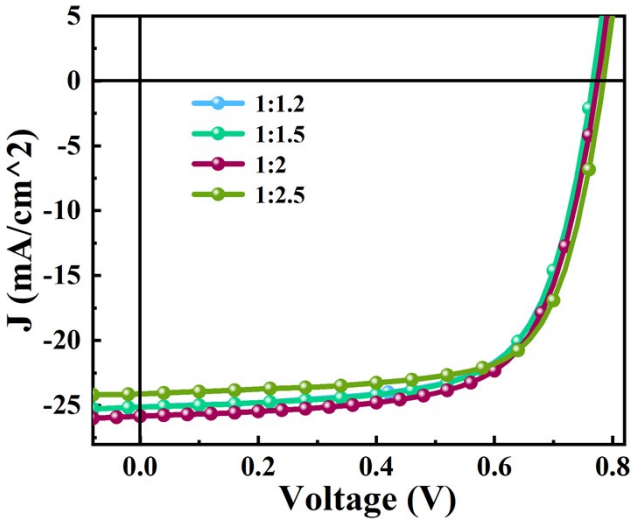

Figure S7. J-V curves of PCE10-2F-53.3kDa: Y6 based solar cells with different D/A ratio with additive of 0.25%DIO and 0.25%CN.

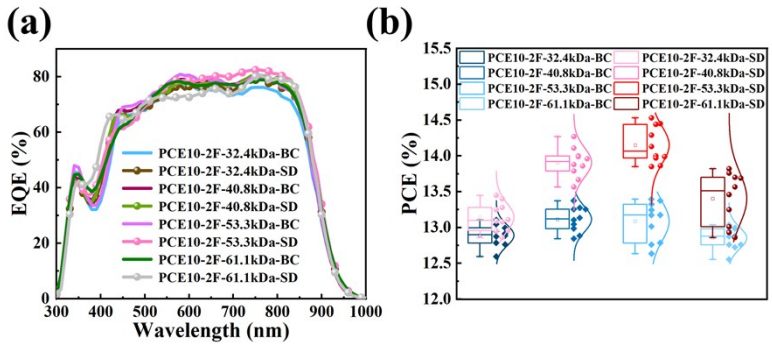

Figure S8. (a) EQE spectra and (b) average PCE of the optimized opaque of the BC and SD OSCs.

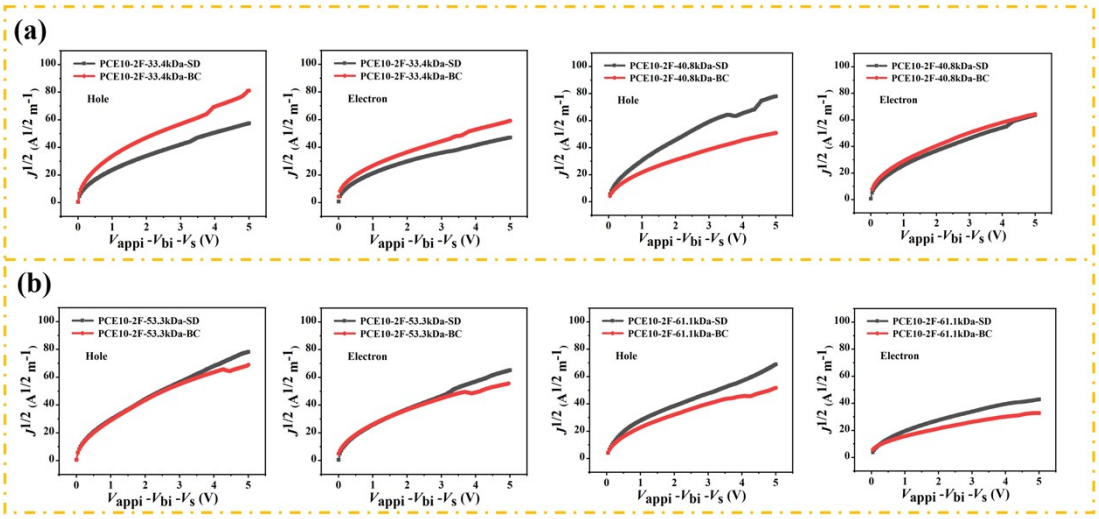

Figure S9. $J^{1/2}$–V plots of hole-only devices and $J^{1/2}$–V plots of electron-only devices (in dark).

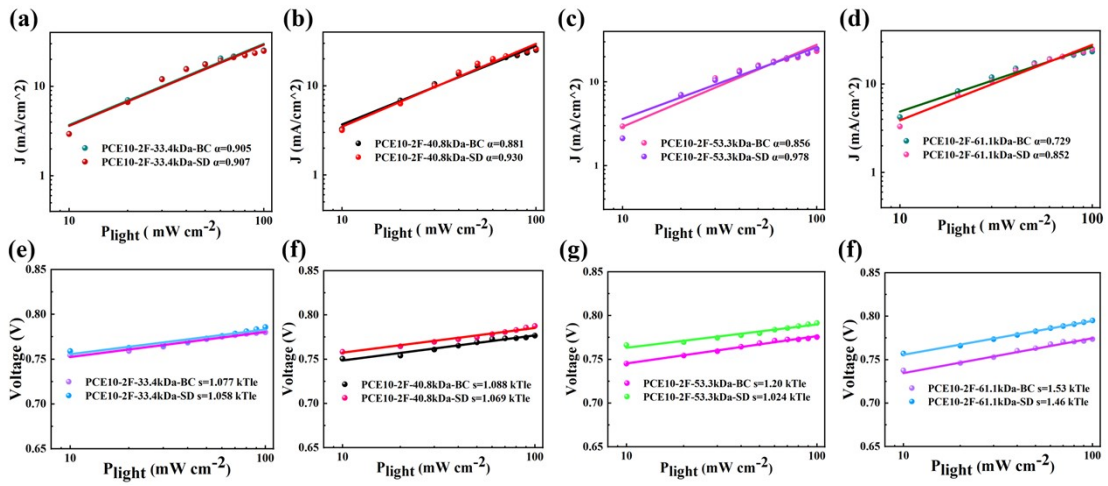

Figure S10. (a-d) Dependence of J_{SC} on the light intensity of the OSC devices. (e-f) Dependence of V_{OC} on the light intensity of the OSC devices.

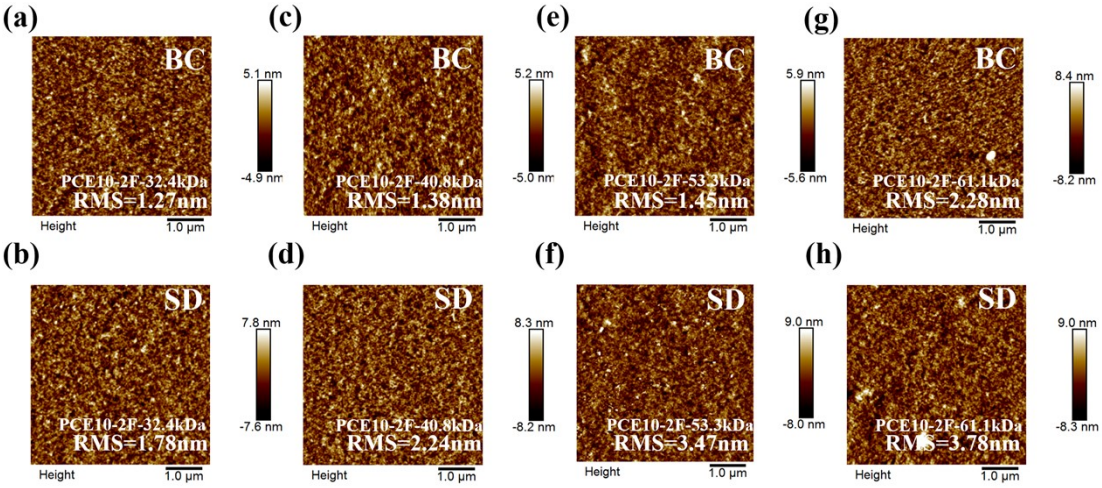

Figure S11.AFM images of optimized BC and SD blend films.

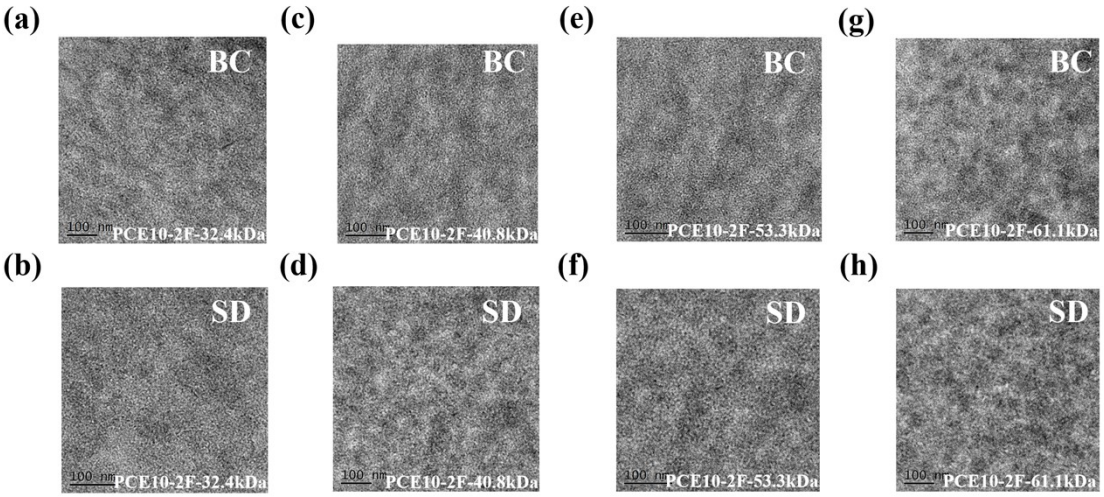

Figure S12. TEM images of optimized BC and SD blend films.

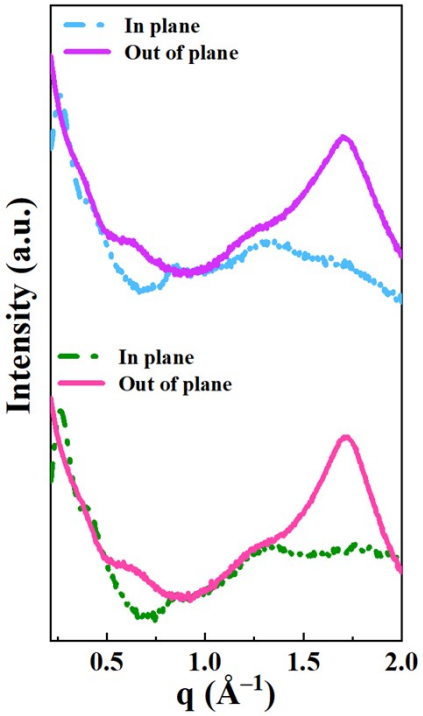

Figure S13. in-plane and out-of-plane line cuts of GIWAXS of the optimized active layers (PCE10-2F-53.3kDa and Y6) based on BC and SD operating conditions.

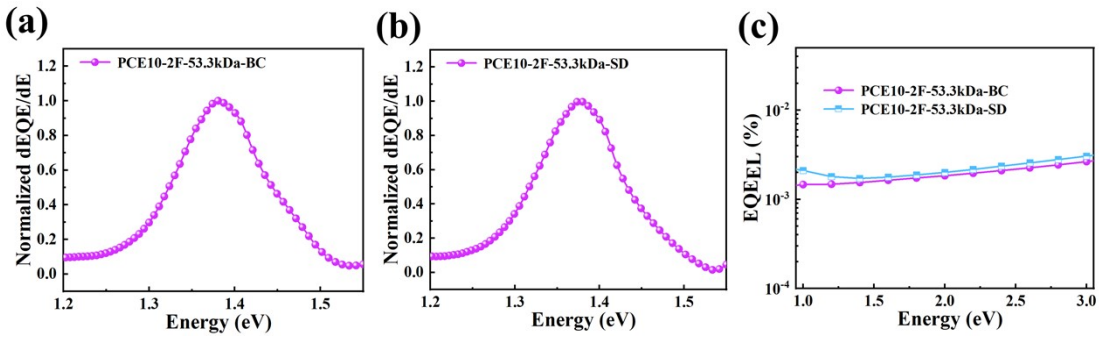

Figure S14. (a-b) Determination of the E_g of the BC and SD operating conditions devices via the derivatives of the EQE spectra, (c) EQE_{EL} of BC and SD devices.

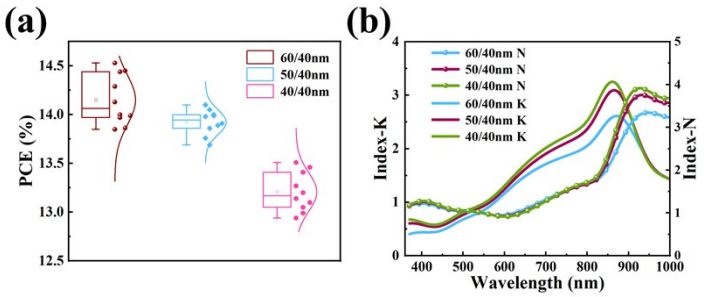

Figure S15. (a) average PCE of the SD processed opaque OSCs with different thickness. Error bars represent the standard deviation of the arithmetic mean of 10 devices. (b) Curves of index-N, K variation with wavelength of the active layer based on different D/A thickness.

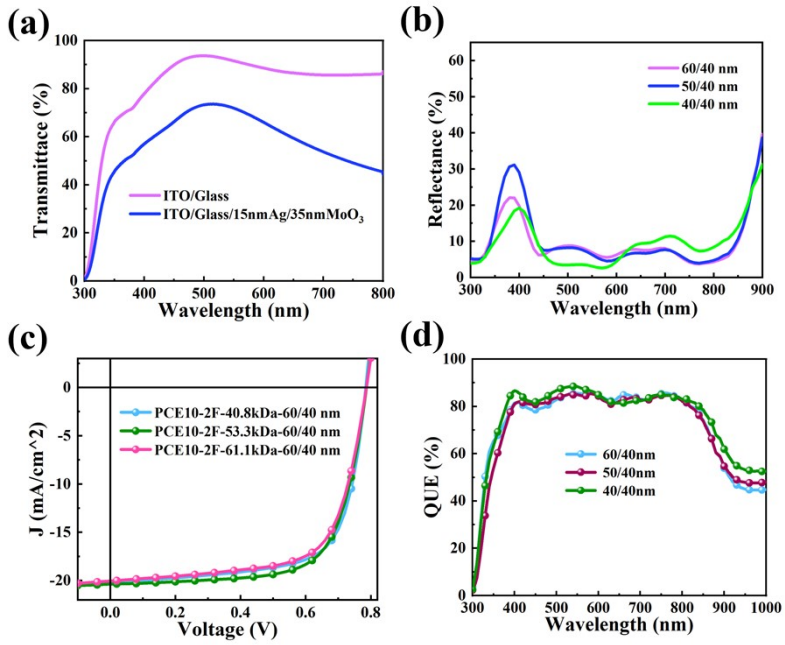

Figure S16. (a) The transmittance of the electrodes and ITO glass used in the device. (b) The reflectance spectrum of ST-OSCs. (c) J-V curves of ST-OSCs based on PCE10-2F with different molecular weight under simulated AM 1.5G, 100 mW cm^{-2} illumination. (d) QUE (EQE+T) curves of the ST-OSCs based on device 60/40nm, 50/40nm, 40/40nm.

Figure S17. Background and ST-OSC filtered photos.

Table S1. Optical and electrochemical parameters of polymer donors.

Polymers	$\lambda_{f,\,max}$ (nm)	$\lambda_{s,\,max}$ (nm)	E_g^{opt} (eV)	λ_f I_{0-0}/I_{0-1}	λ_s I_{0-0}/I_{0-1}	HOMO (eV)	LUMO (eV)
PCE10-2F-33.4kDa	695	699	1.60	1.182	1.300	-5.47	-3.87
PCE10-2F-40.8kDa	697	700	1.59	1.243	1.398	-5.46	-3.87
PCE10-2F-53.3kDa	704	701	1.58	1.324	1.418	-5.45	-3.87
PCE10-2F-60.8kDa	705	701	1.57	1.341	1.440	-5.44	-3.87

Table S2. Summarized parameters for the ordering structures of neat films and blend films.

	Out-of-Plane				In-Plane			
	π-π stacking cell axis (010)				Unit cell long axis (100)			
	q ($Å^{-1}$)	d-spacing (Å)	FWHM ($Å^{-1}$)	Coherence length (Å)	q ($Å^{-1}$)	d-spacing (Å)	FWHM ($Å^{-1}$)	Coherence length (Å)
33.4 kDa	1.606	3.912	0.581	9.845	0.259	24.259	0.105	48.345
40.8 kDa	1.612	3.898	0.476	12.017	0.258	24.353	0.104	42.686
53.3 kDa	1.614	3.893	0.457	12.516	0.258	24.353	0.103	48.764
61.1 kDa	1.616	3.888	0.420	13.620	0.258	24.353	0.102	46.575
Y6	1.708	3.679	0.234	24.44	0.287	21.893	0.234	34.685
Y6+additive	1.764	3.562	0.149	38.396	0.208	30.207	0.155	56.234
BC	1.700	3.696	0.310	18.452	0.262	23.982	0.0874	32.534
SD	1.710	3.674	0.288	19.861	0.264	23.800	0.245	57.754

Table S3. Photovoltaic performance of PCE10-2F-53.3kDa: Y6 based solar cells with different D/A ratio with additive of 0.25%DIO and 0.25%CN.

D/A	V_{OC} (V)	J_{SC} (mA/ cm^2)	FF (%)	PCE_{max} (%)
1:1.2	0.768	25.12	67.34	12.98
1:1.5	0.766	25.13	67.71	13.03
1:2	0.775	25.82	67.07	13.40
1:2.5	0.784	24.11	70.27	13.29

Table S4. Detailed parameter on PCE10 or named PTB7-Th in IC-based non-fullerene organic solar cells devices reported in the literature.

Acytive layer	V_{OC} (V)	J_{SC} (mA/ cm^2)	FF (%)	PCE$_{max}$ (%)	Reference
PCE10-2F/Y6	0.789	26.14	70.32	14.53	This work
PTB7-th: ATT-9	0.66	30.0	67.2	13.35	1
PCE10-BDT2F-0.8: Y6	0.753	26.36	69.45	13.80	2
PCE10-2Cl: IT-4F	0.82	18.13	71.94	10.72	3
PTB7-th: CO*i*8DFIC	0.69	27.3	71	13.8	4
PBTT: IEICO	0.86	17.9	61.3	9.5	5
PBClT: ITIC	1.01	13.95	60.05	8.46	6
PBFTT: IT-4Cl	0.76	19.7	73.9	11.1	7
PTB7-Th: H3	0.780	25.26	67.38	13.38	8
PL-Cl: F8IC	0.71	26.27	69.2	12.9	9
PCE10: A078	0.75	24.8	0.7	13.0	10
PTB7-Th: FOIC	0.743	24.0	67.1	12.0	11
PTB7-Th: FOIC: $PC_{71}BM$	0.753	23.83	66.5	12.32	12
PCE-10: BT-CIC: TT-FIC	0.68	23.3	72	11.4	13
PTB7-Th: IEICO-4F	0.712	27.3	65.7	12.8	14
PTB7-Th: IEICO-4Cl	0.727	22.8	62	10.3	15
PTB7-Th: IUIC	0792	21.51	64.7	11.2	16
PTB7-Th: COi8DFIC: IEICO-4F	0.714	23.97	69.78	11.94	17
PTB7-Th: ACS8	0.75	25.3	69.3	13.2	18
PCE10: ICBA: Y8	0.742	23.51	73.74	12.84	19
PTB7-Th: FNIC1	0.741	23.93	73.4	13.0	20
PTB7-Th: FNIC2	0.774	19.97	66.4	10.3	20
PTB7-Th: ATT-2	0.73	20.75	63	9.58	21

Table S5. Hole and electron mobilities of BC and SD operating conditions devices in the dark.

	Operating conditions	μ_h(cm^2 V^{-1} s^{-1})	μ_e(cm^2 V^{-1} s^{-1})	μ_h/μ_e
PCE10-2F-33.4kDa	BC	8.49×10^{-4}	6.45×10^{-4}	1.38
	SD	9.20×10^{-4}	7.72×10^{-4}	1.19
PCE10-2F-40.8kDa	BC	8.95×10^{-4}	7.18×10^{-4}	1.25
	SD	1.02×10^{-3}	9.38×10^{-4}	1.09
PCE10-2F-53.3kDa	BC	9.67×10^{-4}	8.21×10^{-4}	1.17
	SD	1.03×10^{-3}	9.67×10^{-4}	1.06
PCE10-2F-61.1kDa	BC	7.95×10^{-4}	5.65×10^{-4}	1.41
	SD	9.64×10^{-4}	8.44×10^{-4}	1.14

Table S6. Operating characteristics of OSCs (PCE10-2F-61.1kDa) with different additive based on BC and SD operating conditions under simulated AM 1.5G, 100 mW cm^{-2} illumination.

Donor	Acceptor	Operating conditions	V_{OC} (V)	J_{SC} (mA/ cm²)	FF (%)	PCE_{max} (%)
-	**0.5%CN**	SD	0.810	23.23	65.88	12.36
0.5%CN	**0.5%CN**	SD	0.812	23.49	66.01	12.59
0.5%DIO	**0.5%CN**	SD	0.798	21.97	62.23	10.93
0.5%CN		BC	0.806	23.87	64.64	12.30
-	**0.5%DIO**	SD	0.788	24.07	68.56	13.07
0.5%DIO	**0.5%DIO**	SD	0.774	24.00	68.79	12.97
0.5%DIO		BC	0.775	24.59	67.65	12.86
-	**0.25%CN+0.25%DIO**	SD	0.794	25.70	67.70	13.82
0.5%DIO	**0.25%CN+0.25%DIO**	SD	0.773	25.18	65.34	12.70
0.25%CN+0.25%DIO		BC	0.773	25.83	65.42	13.04

Table S7. Detailed parameter on state-of-the-art ST-OSC devices with complex optical engineering reported in the literature.

Device structure	PCE (%)	AVT (%)	LUE (%)	Reference
$(LiF/TeO2)^4$/glass/ITO/PEDOT:PSS/PM6:BTP-eC9:L8-BO(0.8:1:0.2)/PDINN/Ag(12nm)/$(LiF/TeO2)^8$/LiF	11.44	46.79	5.35	22
MgF_2 /SiO_2 /ITO/ZnO/PCE-10: A078/MoO_3/Ag(16nm)/CBP/MgF_2/CBP/MgF_2	10.8	45.7	5.0	10

Table S8. Detailed parameter on state-of-the-art ST-OSC devices without complex optical engineering reported in the literature.

Acytive layer	PCE (%)	AVT (%)	LUE (%)	Reference
PCE10-2F/Y6 (60/40nm)	11.11	39.93	4.48	This work
PCE10-2F/Y6 (50/40nm)	10.56	45.62	4.82	This work
PCE10-2F/Y6 (40/40nm)	10.01	50.05	5.01	This work
PBDB-TF:L8-BO:BTP-eC9	12.95	38.67	5.0	23
PTB7-Th: H3	8.38	50.9	4.27	8
PTB7-Th: FOIC: $PC_{71}BM$	8.66	50.04	4.33	12
PL-Cl: F8IC	11.0	35.0	3.85	9
PTB7-Th: FOIC	10.3	37.4	3.85	11
PBT1-C-2Cl: Y6	9.1	40.1	3.65	24
PCE-10: BT-CIC: TT-FIC	8.0	44.2	3.54	13
PTB7-Th: IEICO-4Cl	8.38	25.7	2.15	15
PTB7-Th: IUIC	10.2	31	3.16	16
PCE-10: BT-CIC	7.1	43	3.05	25
PTB7-Th: ATT-2	7.7	37	2.85	21
PBDB-T: ITIC	7.3	25.2	1.84	26
PTB7-Th: IHIC	9.77	36	3.52	27
PTB7-Th: COi8DFIC: IEICO-4F	8.23	20.78	1.71	17
PBDTTT-ET: IEICO	6.8	25.1	1.71	28

PTB7-Th: PBT1-S: PC71BM	9.2	20	1.84	29
PBDB-T-2F: Y6	12.88	25.6	3.30	30
PTB7-Th: ACS8	11.1	28.6	3.17	18
PTB7-Th: BDTThIT-4F: IEICO-4F	9.40	24.6	2.31	31
PTB7-Th: IEICO-4F	9.06	27.1	2.46	32
PTB7-Th: IEICO-4F	10.03	34.2	3.43	33
PBDB-T: Y14	12.67	23.69	3.00	34
PBFTT: IT-4Cl	9.1	27.6	2.51	7
PFTzTT3TC: ITIC	6.43	26.77	1.72	35
PBN-S: IT-4F	9.83	32	3.15	36
PTB7-Th: IEICO-4F	10.83	29.5	3.19	37
PDTP-DFBT: FOIC	4.2	52	2.18	38
J71:PTB7-Th: IHIC	9.3	21.4	2.01	39
DTG-IW: PTB7-Th	6.19	50.4	3.12	40
PM6: Y6: PC71BM	10.2	28.6	2.92	41
PBDB-TF: Y6: BTTPC	13.1	22.35	2.93	42
PBDB-TF: Y6: DTNIF	13.49	22.58	3.05	43
PBDB-TF: Y6: PC71BM	13	21.4	2.78	44
PCE10: ICBA:Y8	10.46	26.56	2.78	19
D18-Cl: Y6-1O: Y6	13.02	20.2	2.63	45
PCE10-2Cl: IT-4F	8.25	33	2.72	3

PM2: Y6-BO	5.9	43.3	2.55	46
PM6: Y6: DIBC	14.00	21.60	3.02	47
PM6: Y6	9.7	42.82	4.15	48
PCE10-BDT2F-0.8: Y6	10.85	41.08	4.46	2
PTB7-Th: ATT-9	9.37	35.5	3.33	1
PM6-Ir1: BTP-eC9: PC71BM	14.09	20.44	2.82	49

Table S9. Operating characteristics of ST-OSCs based on PCE10-2F with different molecular weight under simulated AM 1.5G, 100 mW cm^{-2} illumination.

Donor	D/A	V_{OC} (V)	J_{SC} (mA/ cm^2)	FF (%)	PCE (%)	AVT (%)	LUE (%)
PCE10-2F-40.8kDa	60/40nm	0.784	20.18	69.25	10.97	40.13	4.40
PCE10-2F-53.3kDa	60/40nm	0.786	20.37	69.48	11.11	39.93	4.44
PCE10-2F-61.1kDa	60/40nm	0.787	20.05	67.25	10.60	37.95	4.02

REFERENCES

[1] W. Liu, S. Sun, S. Xu, H. Zhang, Y. Zheng, Z. Wei and X. Zhu *Adv. Mater*., 2022, **18**, 2200337.

[2] X. Huang, L. Zhang, Y. Cheng, J. Oh, C. Li, B. Huang, L. Zhao, J. Deng, Y. Zhang, Z. Liu, F. Wu, X. Hu, C. Yang, L. Chen, Y. Chen, *Adv. Funct. Mater*. 2022, **32**, 2108634.

[3] X. Huang, J. Oh, Y. Cheng, B. Huang, S. Ding, Q. He, F. Wu, C. Yang, L. Chen and Y. Chen, *J. Mater. Chem*. A, 2021, **9**, 5711-5719.

[4] W. Li, M. Chen, J. Cai, E. L.K. Spooner, H. Zhang, R. S. Gurney, D. Liu, Z. Xiao, D. G. Lidzey, L. Ding and T. Wang, *Joule*, 2019, **3**, 819-833.

[5] G. Li, W. Li, X. Guo, B. Guo, W. Su, Z. Xu, M. Zhan, *Org. Electron.*, 2019, **64**, 241-246.

[6] P. Chao, Z. Mu, H. Wang, D. Mo, H. Chen, H. Meng, W. Chen and F. He, *ACS Applied Energy Materials*, 2018, **1**, 2365-2372.

[7] W. Su, Q. Fan, X. Guo, J. Wu, M. Zhang and Y. Li, *Phys. Chem. Chem. Phys*., 2019, **21**, 10660-10666.

[8] Y. Li, C. He, L. Zuo, F. Zhao, L. Zhan, X. Li, R. Xia, H.L. Yip, Li, C.Z., X. Liu, and H. Chen, *Adv. Energy Mater*., 2021,**11**, 2003408.

[9] Y. Chang, X. Zhu, L. Zhu, Y. Wang, C. Yang, X. Gu, Y. Zhang, J. Zhang, K. Lu, X. Sun and Z. Wei, *Nano Energy*, 2021, **86**, 106098.

[10] Y. Li, X. Guo, Z. Peng, B. Qu, H. Yan, H. Ade, M. Zhang and S. R. Forrest, *P.N.A.S.* 2020, **117**, 21147.

[11] T. Li, S. Dai, Z. Ke, L. Yang, J. Wang, C. Yan, W. Ma, and X. Zhan, *Adv. Mater*. 2018, **30**, 1705969.

[12] Q. Liu, L.G. Gerling, F. Bernal-Texca, J. Toudert, T. Li, X. Zhan, and J. Martorell, *Adv. Energy Mater*., 2020, **10**, 1904196

[13] Y. Li, C. Ji, Y. Qu, X. Huang, S. Hou, C.Z. Li, L.S. Liao, L.J. Guo and S.R. Forrest, *Adv. Mater*., 2019, **31**, 1903173.

[14] X. Song, N. Gasparini, L. Ye, H. Yao, J. Hou, H. Ade and D. Baran, *ACS Energy Lett.*, 2018, **3**, 669-676.

[15] Y. Cui, C. Yang, H. Yao, J. Zhu, Y. Wang, G. Jia, F. Gao and J. Hou, *Adv. Mater*., 2017, **29**, 1703080. 2.

[16] B. Jia, S. Dai, Z. Ke, C. Yan, W. Ma and X. Zhan, *Chem. Mater*., 2017, **30**, 239-245.

[17] X. Ma, Z. Xiao, Q. An, M. Zhang, Z. Hu, J. Wang, L. Ding and F. Zhang, *J. Mater. Chem. A,* 2018, **6**, 21485-21492.

[18] J. Chen, G. Li, Q. Zhu, X. Guo, Q. Fan, W. Ma, and M. Zhang, *J. Mater. Chem. A*, 2019, **7**, 3745-3751.

[19] C. Zhu, H. Huang, Z. Jia, F. Cai, J. Li, J. Yuan, L. Meng, H. Peng, Z. Zhang, Y. Zou, and Y Li., *Sol Energy,* 2020, **204**, 660-666.

[20] J. Wang, J. Zhang, Y. Xiao, T. Xiao, R. Zhu, C. Yan, Y. Fu, G. Lu, X. Lu, S. R. Marder and X. Zhan, *J. A. C. S*., 2018, **140**, 9140-9147.

[21] F. Liu, Z. Zhou, C. Zhang, J. Zhang, Q. Hu, T. Vergote, F. Liu, T.P. Russell, and X. Zhu, *Adv. Mater*., 2017, **29**, 1606574.

[22] X. Liu, Z. Zhong, R. Zhu, J. Yu and G. Li, *Joule*, 2022, **6**, 1–13.

[23] S. Guan, Y. Li, K. Yan, W. Fu, L. Zuo and H. Chen, *Adv. Mater*., https://doi.org/10.1002/adma.202205844.

[24] Y. Xie, Y. Cai, L. Zhu, R. Xia, L. Ye, X. Feng, H.L. Yip, F. Liu, G. Lu, S. Tan, and Y. Sun, *Adv. Funct. Mater*., 2020, **30**, 2002181.

[25] Y. Li, J.D. Lin, X. Che, Y. Qu, F. Liu, L.S. Liao and S.R. Forrest, *J. Am. Chem. Soc*., 2017, **139**, 17114-17119.

[26] M.B. Upama, M. Wright, N.K. Elumalai, M.A. Mahmud, D. Wang, C. Xu and A. Uddin, *ACS Photonics,* 2017, **4**, 2327-2334.

[27] W. Wang, C. Yan, T.K. Lau, J. Wang, K. Liu, Y. Fan, X. Lu and X. Zhan, *Adv. Mater.,* 2017, **29**, 1701308.

[28] C. Sun, R. Xia, H. Shi, H. Yao, X. Liu, J. Hou, F. Huang, H.-L. Yip and Y. Cao, *Joule,* 2018, **2**, 1816-1826.

[29] Y. Xie, L. Huo, B. Fan, H. Fu, Y. Cai, L. Zhang, Z. Li, Y. Wang, W. Ma, Y. Chen,and Y. Sun, *Adv. Funct. Mater*. 2018, **28**, 1800627.

[30] Y. Bai, C. Zhao, X. Chen, S. Zhang, S. Zhang, T. Hayat, A. Alsaedi, Z.a. Tan, J. Hou and Y. Li, *J. Mater. Chem. A,* 2019, **7**, 15887-15894.

[31] Z. Hu, J. Wang, Z. Wang, W. Gao, Q. An, M. Zhang, X. Ma, J. Wang, J. Miao, C. Yang, and F. Zhang, *Nano Energy*, 2019, **55**, 424-432.

[32] Z. Hu, Z. Wang and F. Zhang, *J. Mater. Chem. A,* 2019, **7**, 7025-7032.

[33] Y. Liu, P. Cheng, T. Li, R. Wang, Y. Li, S.Y. Chang, Y. Zhu, H.W. Cheng, K.H. Wei, X. Zhan, B. Sun and Y. Yang, *ACS Nano*, 2019,**13**, 1071-1077.

[34] M. Luo, C. Zhao, J. Yuan, J. Hai, F. Cai, Y. Hu, H. Peng, Y. Bai, Z.a. Tan and Y. Zou, *Mater. Chem. Front*., 2019, **3**, 2483-2490.

[35] X. Wang, K. Zhu, X. Jing, Q. Wang, F. Li, L. Yu and M. Sun, *ACS Appl. Energy Mater*, 2019, **3**, 915-922.

[36] Y. Wu, H. Yang, Y. Zou, Y. Dong, J. Yuan, C. Cui and Y. Li, *Energy Environ. Sci*., 2019, **12**, 675-683.

[37] R. Xia, C.J. Brabec, H.-L. Yip and Y. Cao, *Joule,* 2019, **3**, 2241-2254.

[38] Y. Xie, R. Xia, T. Li, L. Ye, X. Zhan, H.L. Yip and Y. Sun, *Small Methods*, 2019, **3**, 1900424.

[39] J. Zhang, G. Xu, F. Tao, G. Zeng, M. Zhang, Y.M. Yang, Y. Li and Y. Li, *Adv. Mater*. 2019, **31**, 1807159.

[40] Y. Cho, T.H. Lee, S. Jeong, S.Y. Park, B. Lee, J.Y. Kim and C. Yang, *ACS Appl. Energy Mater*. 2020, **3**, 7689-7698.

[41] B.H. Jiang, H.E. Lee, J.H. Lu, T.H. Tsai, T.S. Shieh, R.J. Jeng and C.P. Chen, *ACS Appl. Mater. Interfaces*, 2020, **12**, 39496-39504.

[42] D. Wang, R. Qin, G. Zhou, X. Li, R. Xia, Y. Li, L. Zhan, H. Zhu, X. Lu, H.L. Yip, H. Chen, C. Li, *Adv. Mater*., 2020, **32**, 2001621.

[43] P. Yin, Z. Yin, Y. Ma and Q. Zheng, *Energy Environ. Sci*., 2020, **13**, 5177-5185.

[44] N. Zhang, T. Jiang, C. Guo, L. Qiao, Q. Ji, L. Yin, L. Yu, P. Murto and X. Xu, *Nano Energy,* 2020, **77**, 105111.

[45] Z. Hu, J. Wang, X. Ma, J. Gao, C. Xu, X. Wang, X. Zhang, Z. Wang and F. Zhang, *J. Mater. Chem. A*, 2021, **9**, 6797-6804.

[46] T. Jiang, G. Zhang, R. Xia, J. Huang, X. Li, M. Wang, H.-L. Yip and Y. Cao, *Mater. Today Energy*, 2021, **21**, 100807.

[47] X. Lu, L. Cao, X. Du, H. Lin, C. Zheng, Z. Chen, B. Sun and S. Tao, *Adv. Opt. Mater*., 2021, **9**, 2100064.

[48] H.I. Jeong, S. Biswas, S.C. Yoon, S.J. Ko, H. Kim and H. Choi, *Adv. Energy Mater*., 2021, **11**, 2102397

[49] W. Liu, S. Sun, S. Xu, H. Zhang, Y. Zheng, Z. Wei, and X. Zhu, *Adv. Mater*., 2022, **34**, 2200337.